Since January 2020 Elsevier has created a COVID-19 resource centre with free information in English and Mandarin on the novel coronavirus COVID-19. The COVID-19 resource centre is hosted on Elsevier Connect, the company's public news and information website.

Available online at www.sciencedirect.com

ScienceDirect

Procedia CIRP 110 (2022) 354–359

www.elsevier.com/locate/procedia

V CIRP Conference on Biomanufacturing

Technological scouting of bi-material face masks: experimental analysis on real faces

Elisa Ficarella[a]*, Angelo Natalicchio[a], Roberto Spina[a], Luigi Maria Galantucci[a]

[a]*Politecnico di Bari, Via Edoardo Orabona 4, 70126, Bari, Italy*

* Corresponding author. Tel.: +39 339 219 1669. *E-mail address:* elisa.ficarella@poliba.it

Abstract

The need for personal protective equipment rapidly grew during the COVID-19. Companies had to face problems related to their products' sustainability, adherence, and comfortability. Designing a face mask with proper adherence and comfortability in wearing and breathing became a matter of great importance. In this work, the adherence of an innovative face mask and its comfortability were experimentally tested with real faces, considering the deformation of the mask and the soft facial tissues. A stereophotogrammetric acquisition was made of the face with the face mask during these tests. A comparison between the geometries of the face and the mask, undeformed and deformed, gave the respective deformations. The force applied by the mask to the face was calculated, measuring the elastic strain of the mask bands during wearing and the deformation.

Keywords: face masks; wearability; COVID-19

1. Introduction

The COVID-19 pandemic led to a shortage in the supply of medical and non-medical products, especially personal protective equipment (PPE) [1–3]. Governments and WHO advised the population that masks dramatically reduced the diffusion of COVID-19 during this pandemic [4–7]. Disposable masks were made with several materials and synthetic polymers, exploring the use of natural-based polymers as valid substitutes [8].

Face masks had a well-established role in mitigating the spread of COVID-19, preventing its symptomatic and asymptomatic transmission [2,3,9]. This condition made these products highly requested worldwide as a healthcare necessity, producing billions. These face masks were created from petrochemicals-derived raw materials, which were non-degradable or reusable, thus affecting and damaging the environment [10]. Another problem caused by the massive use of face masks, especially for health workers, was associated with the comfort of wearing a mask. Surgical masks and FFP2/N95 face masks caused discomfort, reducing ventilation and cardiopulmonary capacity [11]. FFP2/N95 adhered better on the face, causing more discomfort but providing the necessary filtering action [12][13]. Considering all the above aspects, producing locally a mask that was also comfortable, wearing and breathing, and sustainable was highly necessary.

In March 2020, Politecnico di Bari launched the project RI.A.PRO (RIconversione Aziendale per la PROduzione di DPI, literally *Corporate reconversion for the PPE production*), supported by the Apulia Region (Italy), in coordination with the other regional universities, to help small and medium-sized enterprises in a conversion process for producing medical and anti-COVID-19 products [14]. The Apulian company New Euroart S.r.l. (Grumo Appula, Bari, Italy) registered for the program. It formalized a specific research project called *Technological scouting, process mapping, and production fluxes optimization to realize bi-material face masks*. The bi-material product, called Lala Mask®, was comfortable, assuring

10.1016/j.procir.2022.06.063

complete facial adherence. The mask consisted of two different polymers chemically joined during a sequential injection molding process. The rigid part of the mask, called *body*, was made in Polypropylene (PP), while the flexible part in contact with the body skin, called *rubber*, was made in Thermoplastic Elastomer (TPE). All materials were of medical grades. It was also fully sanitizable and washable with soaps and alcohol, hypoallergenic and recyclable. Additional features were extreme lightness and high breathability [15]. The design of this mask was verified by the simulation of adherence using artificial faces generated from 3D Facial Norms, as presented in previous work [16].

2. Photogrammetric scan of masks and faces

2.1. Dimensional analysis of the mask

The first step of the experimental campaign consisted of dimensional analysis of the mask, whose design was a prototype, to obtain a 3D model using photogrammetric scans. The scanned model of the product made through an injection molding process [19] was compared with the original CAD model. The mask was first opacified with special non-toxic sprays. The acquisitions were made with a scanning system composed of three synchronized cameras. Due to the geometry of the masks, two separate acquisitions were necessary (upper and bottom). The acquisitions were processed in Photoscan (Agisoft LLC, St. Petersburg, Russia) [17] and then imported into the Geomagic Wrap (3D systems Corp., Rock Hill, USA) [18] to obtain a watertight 3D model (Fig. 1).

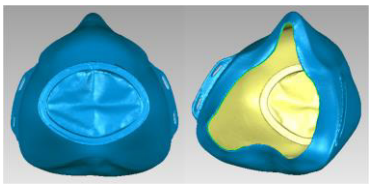

Fig. 1. Final 3D model, front (left figure) and rear (right figure) view

Geomagic Control was later used for quality control and dimensional inspection by comparing the scan and the CAD model (Fig. 2). The files were imported and aligned after defining the *Reference* (reference data, attributed to the photogrammetric scan) and the *Test* (data to be measured, attributed to the CAD). The results showed large areas where the distances between the two models were high because of variations in the CAD and the presence of flexible parts, having multiple dimensional configurations.

2.2. Scanning faces with FaceScanner

The face-scanning was carried out with the equipment and software realized by Polishape 3D srl (Bari, Italy), a spin-off of the Polytechnic of Bari [20–25]. Six individuals of different gender, ages, weight, and height were involved in this study (Table 1). The scanning system was FaceShape Maxi Line, a high-end facial scanner using six high-definition reflex cameras. The multi-camera configuration simultaneously captured frames from different angles.

Table 1. The physical characteristics of the six individuals.

Sex	Men			Women		
ID	#1	#2	#3	#4	#5	#6
Age [y]	25	25	26	24	31	29
Weight [kg]	67	68	70	43	54	60
Height [m]	1.72	1.75	1.78	1.52	1.67	1.58

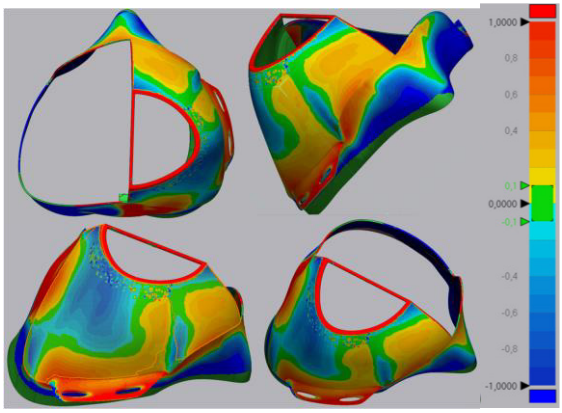

Fig. 2. The 3D comparisons between CAD and scans in mm.

The six cameras were fixed to an aluminum shelf containing the power supplies, control electronics, cables, and coupling systems. The Poliscan software, implemented by the same company, managed the acquisitions. After opacifying the mask with non-harmful products, colored notches were marked on the elastics for subsequent measurements. Therefore, four acquisitions were made for each subject: one frontal before wearing the mask and three without (one frontal and two laterals). Finally, the images were processed in Photoscan [17] to obtain the 3D models (Fig. 3).

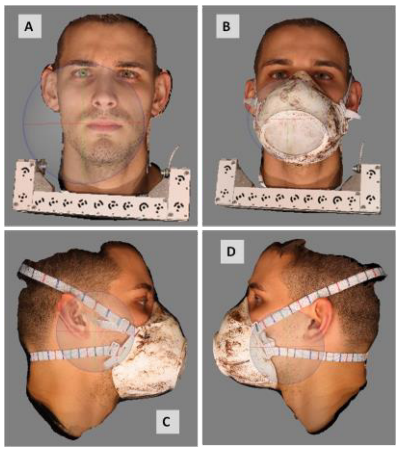

Fig. 3. a) Frontal subject #2 without the mask, b) Frontal view, c) Right lateral view, and d) Left lateral view of subject #2 with the mask

Since FaceScanner did not scan subjects up to 360°, three separate acquisitions were performed for each subject (one front and two laterals) to detect cheekbones and lateral areas of the elastics. The three partial models were combined into a single face reconstruction after the reference collar and other unnecessary parts were digitally removed. The alignment of the models was carried out first with the *Manual Registration* command with four points by setting the front one as the fixed set and the lateral models as floating sets.

Fig. 4. Merged models of the six individuals with the mask

Before executing the merge, the *Global Registration* command (ICP) was performed. The forehead was selected as the sampling area, as it remained unchanged. During these operations, the standard deviation and the average distance were checked to be under 0.1 mm. Fig. 4 shows the final models of the six individuals.

3. Detection of deformations

3.1. Analysis of face deformations

The models of the faces with and without masks were compared (Fig. 5 and 6), after selecting the parameters for the comparison (Table 2).

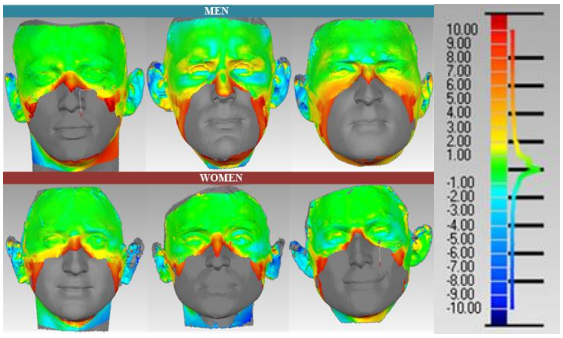

Fig. 5. 3D comparison with and without the mask (frontal view) in mm.

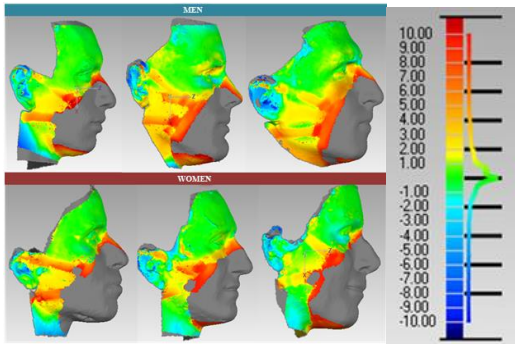

Fig. 6. 3D comparison with and without the mask (lateral view) in mm.

Table 2. Parameters of 3D comparisons.

Parameter	Max and Min deviation	Critical Angle	Critical max and min	Nominal max and min
Value	±9.89 mm	45°	±10 mm	±1 mm

The models were placed in the same analysis condition using an equivalent cutting plane to correctly detect the deformed part of the face (red color of the colorimetric map). Since the six subjects had different facial geometries, each section plane's specific coordinates were entered to evaluate the same zygomatic area. The section curves of both the deformed and non-deformed models were determined (Fig. 7), and the deviation between the two geometries was displayed. Labels *DEF.1-DEF.4* were assigned to four points to select the same face areas for all subjects.

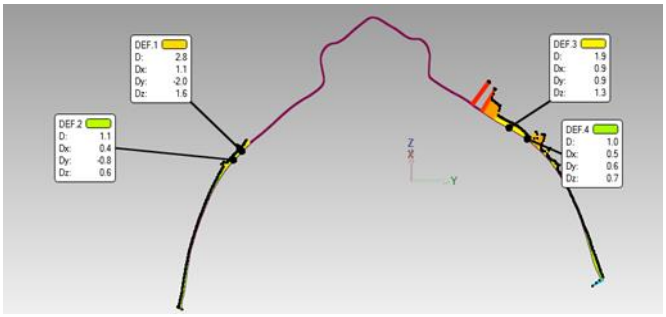

Fig. 7. Result of 2D comparison on subject #1 and points of soft tissue deformation (all dimensions in mm)

3.2. Deformation of the facemasks

In the study of the model deviation, the mask before wearing (not subject to deformation) was chosen as the *Reference*, while the *Test* was attributed to the worn mask. The latter was selected and cut from the faces of the subjects using the *Selection* tools. The two meshes were aligned using the *Manual Registration* and *Global Registration* commands, identifying the rigid part of the template as the sampling area. The parameters for the 3D comparisons were set as in the previous analysis. Fig. 8 shows one of the 3D comparisons made.

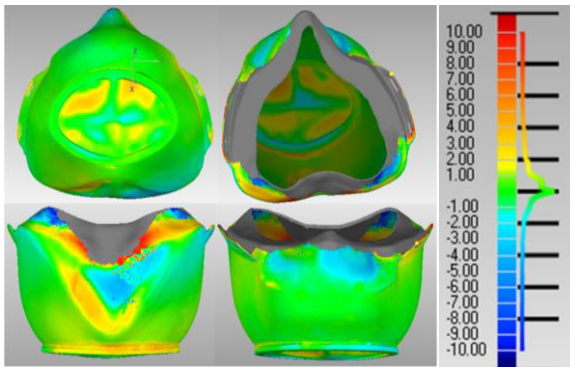

Fig. 8. Colour map and spectrum of deviations of the 3D comparison between the worn and unworn mask in mm.

The rigid part of the mask, called *body*, was not subject to deformation due to its lower flexibility. The seal of the flexible part, called *rubber*, was not visible when the mask was worn, acquiring with photogrammetric techniques not possible. Using the same procedure applied for the faces, a cutting plane for each model was defined with the identical coordinates of the 2D comparison of the soft tissues. The section curves of the deformed and the non-deformed masks were determined (Fig. 9).

Fig. 9. Result of the 2D comparison of the mask worn by subject #1 and points of deformation.

Labels *P.1-P.4* were assigned to four points to consider the same face areas for all subjects.

4. Tensile tests of the elastics

4.1. Implementation of the measurement system

The deformations were closely related to the tension of the elastic bands of the mask. Thus, it was necessary to define a method for measuring the force and load exerted on the face. Tensile tests were carried out on the elastics. First, the elastics were marked with uniformly spaced notches with the help of a custom-made template. The initial distance between the notches in the absence of load was equal to 9.47 mm. Secondly, a structure consisting of aluminum profiles was created to perform the tests. At one end, the elastic was constrained, applying weight on the opposite side. A measuring device was inserted into the structure. Finally, as for the template, the housing was designed, and 3D printed for the weights ranging between 10 and 500 grams, connecting them to the elastic's free end. A weight of 20 grams was set in the housing printing phase and subsequently verified and considered during the tensile tests.

4.2. Tensile behavior of elastomers

To establish a method to adopt, various preliminary tests were carried out to evaluate the tensile mechanical behavior of the elastic bands. At first, to understand the maximum value of the load, the distances between two consecutive notches on the elastics were measured to identify the maximum stretch occurring when the mask was worn. For the measurements, three areas were chosen: *A1*, closer to the mask; *A3*, closer to the ears; and *A2*, intermediate (Fig. 10). The measurements were made on each model on both sides using the *Distance tool* function of Geomagic Control, and a maximum distance of 19.03 mm was found.

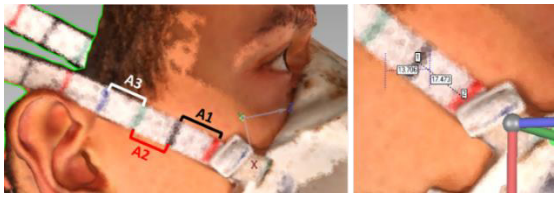

Fig. 10. Identification of areas A1, A2, and A3 and measurement of the distance between two marks with Geomagic Control.

Then, a tensile test with an incremental load of 10 grams was carried out to define the weight range during the measurements. The weight to obtain values of 19 mm was 360 grams. At the end of the first test, the plastic deformation of the material was identified. Measurements were also performed during weight unloading to record the force-elongation hysteresis. The procedure for loading and unloading consisted of a load variation of 30 grams up to the maximum value of 360 grams in the loading and 0 grams in unloading.

4.3. Tensile test results

A sample consisting of three elastics was tested, and, on each one, three repetitions were performed to make further assessments on degradation. Each repetition can be attributed to the number of times a subject wears the mask. For the first repetition, the result is reported in Fig. 11, showing a hysteresis.

Since the subjects wore the mask only once, the hysteresis of the first repetition was considered, causing a more significant deformation. Fig. 11 shows the logarithmic trend line added, which better overlapped the traction curve (R^2 = 0.9977). Equation (1) calculated the force associated with the distances measured with Geomagic on the mask elastics.

$$y = 5.112\,ln(x) - 11.375 \quad \text{(mm)} \tag{1}$$

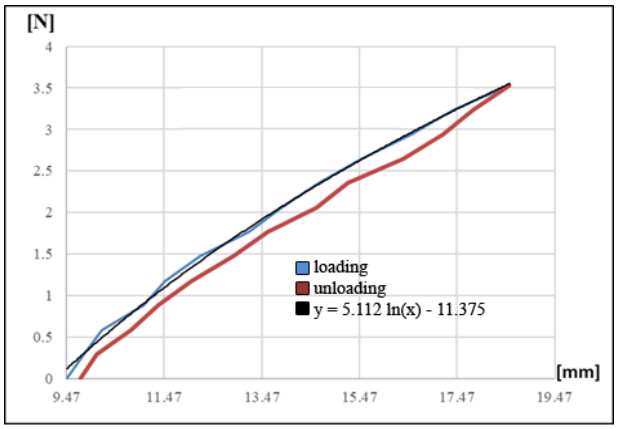

Fig. 11. Force vs. elongation for the first repetition compared with the logarithmic curve.

5. Results and discussion

For each subject, the points *DEF.1*, *DEF.2*, *DEF.3, DEF.4* were detected on the areas of deviation between the section curves on the zygomatic area of the meshes with and without a mask. The face areas in contact with the mask were considered, and significant deformation was assumed (Table 3).

Table 3. Soft tissue deformation points

Sex	ID	Deformation of soft tissue [mm]			
		DEF.1	*DEF.2*	*DEF.3*	*DEF.4*
Men	1	2.80	1.10	1.90	1.00
	2	2.39	0.83	2.93	1.85
	3	3.22	0.98	3.31	1.19
Women	4	1.74	0.27	1.44	0.61
	5	3.47	3.33	3.48	1.93
	6	3.41	2.46	0.68	0.39

It was possible to note that:

- *DEF.1* (left cheekbone area) and *DEF.3* (right cheekbone area) had the highest values because closing to the contact area with the mask edges. Except for subject #1, there were no differences between the deformations of the right and left sides.
- *DEF.2* (left zygomatic area) and *DEF.4* (right zygomatic area) assumed the lowest values, as they were further away from the contact area with the mask edges. There were no notable differences between right and left-sided deformations, except for subject #6.

Based on the above results, only the deformations *DEF.1* and *DEF.3* were investigated in the subsequent analyses. Only the *A1* area closer to the mask was evaluated for the calculated force. Table 4 summarizes the experimental data relating to the relationship between the force values exerted by the elastics and the deformation of the soft tissues. A greater deformation did not always correspond to a greater force because the skin behavior was linked to aspects of dermatological nature specific to the individual.

Table 4. Deformation and strength data.

ID	Skin deformation [mm]		Upper elastic force [N]		Lower elastic force [N]	
	DEF.1	*DEF.3*	Left	Right	Left	Right
1	2.80	1.90	2.36	3.25	0.47	0.81
2	2.39	2.93	2.55	3.69	1.06	1.16
3	3.22	3.31	3.29	3.58	1.26	1.23
4	1.74	1.44	2.26	2.22	0.68	0.93
5	3.47	3.48	2.87	2.99	0.56	0.70
6	3.41	0.68	2.28	2.56	1.07	0.70

Comparing individuals based on gender, the three men (subjects #1, #2, #3) had deformations like those of the female subjects #5 and #6. Gender did not notably influence deformation [26]. The differences between men and women could be significant for the mask deformation, as it varied according to the geometry. Generally, female faces were smaller, and recommending a standard mask size could not suit the entire population [27]. The more problematic area for the contact was located under the chin. In the upper zygomatic region, the high deformation in female subjects was not due to a better mask fit. Significant differences were detected for female subject #4, attributable to other factors such as her low weight and a low thickness between the soft and hard tissues. The weight could be recognized as one of the most influencing factors on the mask wearability. The same assessments could be extended to the height as it was typically related to weight. However, the weight and soft tissue deformations were not always directly proportional. The three men had similar weights (and heights), different from the women. Nevertheless, they presented smaller deformation values. Another leading cause could be the chronological age since subjects #5 and #6 were the oldest. Their more significant deformation could reduce skin elasticity [28]. The analysis of the male ages confirmed this evaluation. The three men were similar, belonging to the same age group (25 and 26 years). The youngest subject had the lowest deformation values (age 24).

As for the faces, four points (*P.1*, *P.2*, *P.3*, *P.4*) were defined on the deviation areas between the section curves of the masks, typical to all individuals. The measurement results are shown in Table 5.

Table 5. Deformation points of masks

	Mask deformation [mm]			
	P.1	*P.2*	*P.3*	*P.4*
1	0.91	2.53	1.05	2.61
2	0.56	2.48	0.66	2.63
3	1.10	2.37	0.65	2.46
4	0.75	2.31	1.79	2.45
5	1.07	2.42	1.19	1.66
6	0.72	2.61	0.67	2.38

In particular:

- Points *P.1* and *P.3* had lower deformation values as they were placed on the rigid part of the mask. No significant differences were recorded between the right and left sides.
- Points *P.2* and *P.4* had high deformation values because they were placed on the flexible gasket of the mask. No significant differences were recorded between the right and left sides.

Minor deformations were observed on the mask of subject 4. As shown in Table 3, the force exerted on the masks worn by women was less than that acting on the masks worn by men. The deformations were of the same order. The elongation of the elastic mainly depended on two factors:

- The comfort level would place all the subjects involved in this study at the same level. The six individuals donned the mask independently and adjusted the length of the elastics according to the desired comfort.
- The size of the head was measured to be greater in men.

6. Conclusions

In this project, deformations of the soft tissues were detected following the use of facemask starting from the 3D models of individuals, equally distributed in gender, of different weights, heights, and ages. Tensile tests on the elastics of the mask were executed. This study helped perform the Finite Element Method. It allowed the mask design to consider the face deformation, improve adaptability, reduce the loss zones on edges, and increase comfort with less skin injury risk.

The results showed that the subject weight and deformations of soft tissues were not always directly proportional. The influence of the age factor on the skin's elasticity should be considered. As regards gender, no substantial differences were found. The analysis could be extended to areas below the chin, where the more problematic zones for the contact are located. Although the deformations of the masks were of the same order of magnitude for all six individuals, the force exerted on those worn by women was less than for men because of head size. Aspects of a dermatological nature, such as the distribution of subcutaneous fat, the elastic modulus, and the thickness of the soft tissues, should be further examined.

Acknowledgments

Joint research was done in the context of RI.A.PRO project of Politecnico di Bari (RIconversione Aziendale per la PROduzione di DPI, literally *Corporate reconversion for the PPE production*) between Politecnico di Bari and New Euroart S.r.l. (Grumo Appula, BA, Italy), who financially supported the research project.

The authors wish to thank Mattia Lala and Federica Rinaldi for their contributions.

References

[1] Cucinotta D, Vanelli M. WHO Declares COVID-19 a Pandemic. Acta Biomed 2020;91:157–60.

[2] Worby CJ, Chang HH. Face mask use in the general population and optimal resource allocation during the COVID-19 pandemic. Nat Commun 2020;11:4049.

[3] Salmi M, Akmal JS, Pei E, Wolff J, Jaribion A, Khajavi SH. 3D printing in COVID-19: Productivity estimation of the most promising open source solutions in emergency situations. Appl Sci 2020;10:1–13.

[4] Das S, Sarkar S, Das A, Das S, Chakraborty P, Sarkar J. A comprehensive review of various categories of face masks resistant to Covid-19. Clin Epidemiol Glob Heal 2021;12:100835.

[5] Forouzandeh P, O'Dowd K, Pillai SC. Face masks and respirators in the fight against the COVID-19 pandemic: An overview of the standards and testing methods. Saf Sci 2021;133:104995.

[6] Ju JTJ, Boisvert LN, Zuo YY. Face masks against COVID-19: Standards, efficacy, testing and decontamination methods. Adv Colloid Interface Sci 2021;292:102435.

[7] Liao M, Liu H, Wang X, Hu X, Huang Y, Liu X, et al. A technical review of face mask wearing in preventing respiratory COVID-19 transmission. Curr Opin Colloid Interface Sci 2021;52:101417.

[8] Mallakpour S, Azadi E, Hussain C. Protection, disinfection, and immunization for healthcare during the COVID-19 pandemic: Role of natural and synthetic macromolecules. Sci Total Environ 2021;776:145989.

[9] Eikenberry SE, Mancuso M, Iboi E, Phan T, Eikenberry K, Kuang Y, et al. To mask or not to mask: Modeling the potential for face mask use by the general public to curtail the COVID-19 pandemic. Infect Dis Model 2020;5:293–308.

[10] Das O, Neisiany ER, Capezza AJ, Hedenqvist MS, Försth M, Xu Q, et al. The need for fully bio facemasks to counter coronavirus outbreaks: A perspective. Sci Total Environ 2020;736:139611.

[11] Finkenzer S, Uhe T, Lavall D, Rudolph U, Falz R, Busse M, et al. Effect of surgical and FFP2/N95 face masks on cardiopulmonary exercise capacity. Clin Res Cardiol 2020;109:1522–30.

[12] Tcharkhtchi A, Abbasnezhad N, Zarbini Seydani M, Zirak N, Farzaneh S, Shirinbayan M. An overview of filtration efficiency through the masks: Mechanisms of the aerosols penetration. Bioact Mater 2021;6:106–22.

[13] Occupational Safety and Health Administration. OSHA Training Video Entitled Respirator Types, <https://www.osha.gov/respiratory-protection/training>; 2020 [accessed 15.02.2022].

[14] Politecnico di Bari. RIAPRO - Riconversione aziendale per la produzione di DPI, <https://www.poliba.it/it/ateneo/riapro-riconversione-aziendale-la-produzione-di-dpi>; 2020 [accessed 15.02.2022].

[15] New Euroart S.r.l. Lala Mask <https://www.lalamask.it/>; 2021 [accessed 15.02.2022].

[16] Ficarella E, Natalicchio A, Spina R, Galantucci LM. Technological scouting of bi-material face masks: simulation of adherence using 3D Facial Norms. In: Ceretti E, Filice L, editors. Procedia CIRP - V CIRP Conf. Biomanufacturing, Vibo Valentia: Elsevier; 2022.

[17] Agisoft LLC. Photoscan, <https://www.agisoft.com/>; 2016 [accessed 15.02.2022].

[18] 3D Systems Corp. Geomagic, <https://www.3dsystems.com/software/geomagic-design-x>; 2013 [accessed 15.02.202].

[19] Laschet G, Spekowius M, Spina R, Hopmann C. Multiscale simulation to predict microstructure dependent effective elastic properties of an injection molded polypropylene component. Mech Mater 2017;105:123–37.

[20] Deli R, Galantucci LM, Laino A, D'Alessio R, Di Gioia E, Savastano C. Three-dimensional methodology for photogrammetric acquisition of the soft tissues of the face: a new clinical-instrumental protocol 2013;14:1.

[21] Galantucci LM, Percoco G, Lavecchia F. A new three-dimensional photogrammetric face scanner for the morpho-biometric 3D feature extraction applied to a massive field analysis of Italian attractive women. Procedia - Soc Behav Sci 2013;5:259–64.

[22] Galantucci LM, Deli R, Laino A, Di Gioia E, D'Alessio R, Lavecchia F, et al. Three-Dimensional Anthropometric Database of Attractive Caucasian Women : Standards and Comparisons 2016;27:1884–95.

[23] Galantucci LM, Percoco G, Lavecchia F, Di Gioia E. Noninvasive computerized scanning method for the correlation between the facial soft and hard tissues for an integrated three-dimensional anthropometry and cephalometry. J Craniofac Surg 2013;24:797–804.

[24] Pesce M, Galantucci LM, Percoco G, Lavecchia F. A Low-cost Multi Camera 3D Scanning System for Quality Measurement of Non-static Subjects. Procedia CIRP 2015;28:88–93.

[25] Deli R, Di Gioia E, Galantucci LM, Percoco G. Accurate facial morphologic measurements using a 3-camera photogrammetric method. J Craniofac Surg 2011;22:54–9.

[26] Cua AB, Wilhelm KP, Maibach HI. Elastic properties of human skin: relation to age, sex, and anatomical region. Arch Dermatol Res 1990;282:283–8.

[27] Solano T, Mittal R, Shoele K. One size fits all?: A simulation frame facemask fit on population-based faces. PLoS One 2021;16:e0252143.

[28] Escoffier C, d. Rigal J, Rochefort A, Pharm M, Vasselet R, LCvCque J-L, et al. Age-Related Mechanical Properties of Human Skin: An in Vivo Study. J Invest Dermatol 1989:353–7.